Non-stationary and non-linear influence of ENSO and Indian Ocean Dipole on the variability of Indian monsoon rainfall and extreme rain events

Jagdish Krishnaswamy, Srinivas Vaidyanathan, Balaji Rajagopalan, Mike Bonell, Mahesh Sankaran, R. S. Bhalla & Shrinivas Badiger

Climate Dynamics
Observational, Theoretical and Computational Research on the Climate System

ISSN 0930-7575
Volume 45
Combined 1-2

Clim Dyn (2015) 45:175-184
DOI 10.1007/s00382-014-2288-0

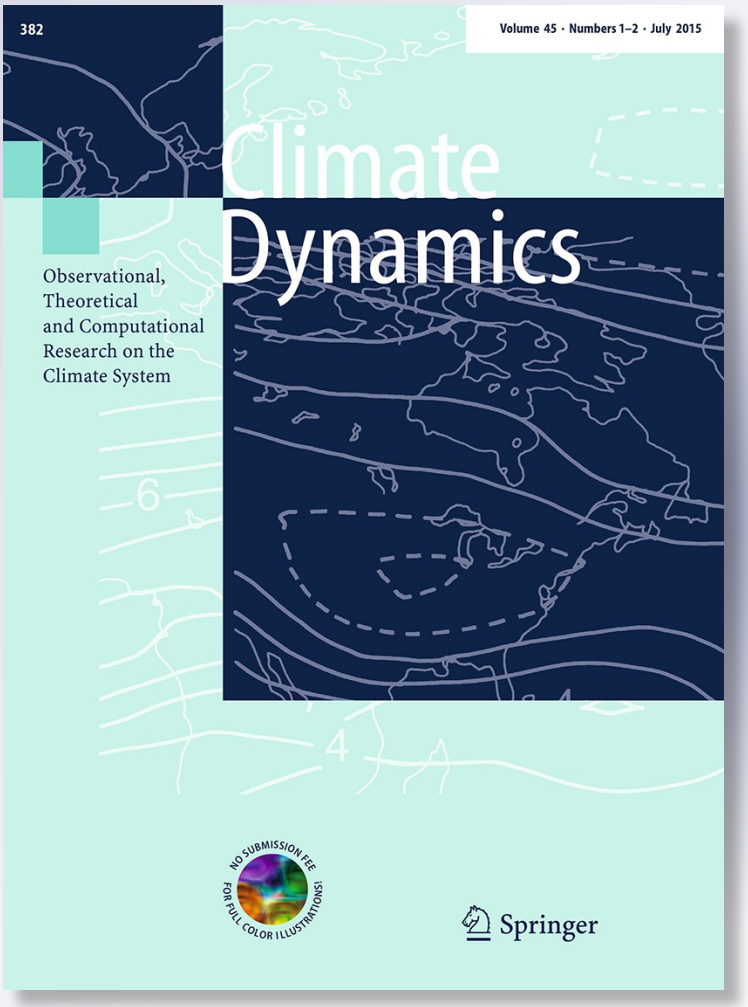

Springer

Clim Dyn (2015) 45:175–184
DOI 10.1007/s00382-014-2288-0

Non-stationary and non-linear influence of ENSO and Indian Ocean Dipole on the variability of Indian monsoon rainfall and extreme rain events

Jagdish Krishnaswamy · Srinivas Vaidyanathan · Balaji Rajagopalan · Mike Bonell · Mahesh Sankaran · R. S. Bhalla · Shrinivas Badiger

Received: 6 March 2014 / Accepted: 5 August 2014 / Published online: 23 August 2014

Abstract The El Nino Southern Oscillation (ENSO) and the Indian Ocean Dipole (IOD) are widely recognized as major drivers of inter-annual variability of the Indian monsoon (IM) and extreme rainfall events (EREs). We assess the time-varying strength and non-linearity of these linkages using dynamic linear regression and Generalized Additive Models. Our results suggest that IOD has evolved independently of ENSO, with its influence on IM and EREs strengthening in recent decades when compared to ENSO, whose relationship with IM seems to be weakening and more uncertain. A unit change in IOD currently has a proportionately greater impact on IM. ENSO positively influences EREs only below a threshold of 100 mm day^{-1}. Furthermore, there is a non-linear and positive relationship between IOD and IM totals and the frequency of EREs (>100 mm day^{-1}). Improvements in modeling this complex system can enhance the forecasting accuracy of the IM and EREs.

Keywords Dynamic linear models · Generalised additive models · La Nina · Western Ghats · Indo-Gangetic plain

1 Introduction

The Indian monsoon (IM) and associated extreme daily rain events (EREs) have a major influence on the welfare of over 1.2 billion people (Gadgil and Kumar 2006; Ashfaq et al. 2009). Variability in the IM is known to be modulated by two ocean–atmosphere phenomena, El Nino–Southern Oscillation (ENSO) and the more recently described Indian Ocean Dipole (IOD; Saji et al. 1999; Ashok et al. 2004). The possible linkages between ENSO and IOD are also an active area of investigation (Wang and Wang 2014).

Earlier studies have shown a weakening ENSO–IM relationship in recent decades attributed to a warmer climate

M. Bonell—Deceased on 11 July 2014.

Electronic supplementary material The online version of this article (doi:10.1007/s00382-014-2288-0) contains supplementary material, which is available to authorized users.

J. Krishnaswamy (✉) · S. Badiger
Ashoka Trust for Research in Ecology and the Environment (ATREE), Royal Enclave Sriramapura, Jakkur Post, Bangalore 560064, Karnataka, India
e-mail: jagdish@atree.org

S. Vaidyanathan · R. S. Bhalla
Foundation for Ecological Research, Advocacy and Learning (FERAL), Pondicherry Campus, 170/3 Morattandi, Auroville Post, Villupuram 605101, Tamil Nadu, India

B. Rajagopalan
Department of Civil, Environmental and Architectural Engineering and Co-operative Institute for Research in Environmental Sciences, University of Colorado, Boulder, CO, USA

M. Bonell
Centre for Water Law, Policy and Sciences Under the Auspices of UNESCO, University of Dundee, Dundee DD1 4HN, Scotland, UK

M. Sankaran
Ecology and Evolution Group, National Centre for Biological Sciences, TIFR, GKVK Campus, Bellary Road, Bangalore 560065, India

M. Sankaran
School of Biology, University of Leeds, Leeds LS2 9JT, UK

(Kumar et al. 1999; Ashrit et al. 2001; Ihara et al. 2008), and a concurrent strengthening of the IOD–IM relationship (Ashok et al. 2001, 2004; Ashok and Saji 2007; Izumo et al. 2010; Ummenhofer et al. 2011) attributed to non-uniform warming of the Indian Ocean (Ihara et al. 2008; Cai et al. 2009). Extreme rainfall events have also simultaneously increased over parts of India (Goswami et al. 2006; Rajeevan et al. 2008; Ghosh et al. 2012) and the same has been linked to global warming and warming of the Indian Ocean (Goswami et al. 2006; Ajaymohan and Rao 2008; Rajeevan et al. 2008). Interestingly, an overall decline in average IM in recent decades has been reported (Kumar et al. 2011; Krishnan et al. 2013). However certain parts of the country are witnessing an increase in average IM (Guhathakurta and Rajeevan 2008) and in the frequency of EREs (Guhathakurta et al. 2011). The possible role of changes in the land-sea temperature gradient which explain these declines have been reported in earlier studies (Han et al. 2010; Kumar et al. 2011; Krishnan et al. 2013). The evolution of monsoon-IOD feedbacks are also well documented (Abram et al. 2008; Vinayachandran et al. 2009; Luo et al. 2010). Although the overall IM is declining, precipitable moisture for sustaining ERE's could be increasing due to local processes (Trenberth et al. 2003) and also due to larger global phenomena such as SSTs in other ocean basins outside the Indo-Pacific sector (Turner and Annamalai 2012; Cherchi and Navarra 2013; Wang et al. 2013). On the other hand, a recent study (Prajeesh et al. 2013) indicates the possibility of a weakened local mid-tropospheric humidity resulting in reduction in monsoon depression frequency.

Previous studies have looked independently at either overall annual monsoon totals or daily rainfall at high exceedance thresholds (such as above 150 mm day^{-1}), rather than as a continuum from low to high and very high exceedance levels. However, the impact of EREs depend on the land-use and land-cover and antecedent moisture status, and thus a daily rainfall of 25 or 50 mm day^{-1} can have an "extreme" impact on people, property, ecosystem response and livelihoods. Existing studies have also addressed changes over time in monsoon and ocean–atmosphere phenomena using moving window correlations, dividing time scale into arbitrary time-periods or linear regression models with time-invariant regression parameters. Most studies, with some exception (Ashok et al. 2001), have focused on specific years, e.g. El Nino, La Nina, positive and negative IOD years, rather than consider the full range of ocean–atmosphere index values to assess their influence on IM and EREs.

There is thus a need for robust methods to model non-stationarity in a continuous and consistent manner across the full range of ocean–atmosphere indices for both Monsoon totals and frequency of EREs across a range of exceedance thresholds with clearly identified parameters that are easy to interpret, along with the quantification of uncertainties. Potential non-linearities in the relationships also need to be identified as the basis for better understanding and forecasting. To this end, we introduce the application of two robust methods to study changes in the relationship between two principal ocean–atmosphere phenomena as well as their evolving influence on monsoon dynamics and annual frequency of EREs at multiple exceedance thresholds over multi-decadal time-scales. We demonstrate that the application of these two methods: *Bayesian dynamic linear regression (DLM) to model non-stationarity based on time-varying regression parameters over multi-decadal scales, and generalized additive models (GAMs) to model non-linearity in the relationships, averaged over larger time periods,* and show how this helps us understand recent shifts and trends in influence of ENSO and IOD on IM and EREs.The scope of this work is primarily to introduce more robust methods for evaluating the impacts of ENSO–IOD on IM extreme rainfall, both for studying and understanding past dynamics as well as for forecasting.

Dynamic state-space models (DLM) including those with time-varying regression parameters (Harrisons and Stevens 1976) have been familiar to statisticians and time-series modellers since the mid-80s when it was applied to economic and industrial output time-series (West et al. 1985; Harrison and West 1997). Dynamic models with time-varying regression coefficients have been used to study changes in stream hydrology and population ecology (Krishnaswamy et al. 2000, 2001; Calder et al. 2003) and more recently to analyze changes in vegetation greenness in response to climate change (Krishnaswamy et al. 2014). Their application in understanding monsoon dynamics in relation to ocean–atmosphere phenomena, however, has been limited (Maity and Nagesh Kumar 2006).

An important statistical development in the last few decades has been advances in GAMs. GAMs (Hastie and Tibshirani 1986, 1990) are semi-parametric extensions of generalized linear models (GLMs), and are based on an assumed relationship (called a link function) between the mean of the response variable and a smoothed, additive, non-parametric function of the explanatory variables rather than a linear function of the covariates as in a GLM.

Data may be assumed to be from several families of probability distributions, including normal, binomial, poisson, negative binomial, or gamma distributions, many of which better fit the non-normal error structures of most ecological and biophysical data. The only underlying assumption made is that the functions are additive and that the components are smooth. The strength of GAMs lies in their ability to deal with highly non-linear and non-monotonic relationships between the response and the set of explanatory variables. GAMs are data rather than model driven. This is because

the data determine the nature of the relationship between the response and the explanatory variables rather than assuming some form of parametric relationship (Yee and Mitchell 1991). Like GLMs, the ability of the method to handle non-linear data structures can aid in the development of models that better represent the underlying data, and hence increase our understanding of biophysical systems. GAMs have been widely used in a range of scientific domains to model non-linearity in regression type data (Lehmann et al. 2002). This provides a better fit to environmental, ecological or meteorological data when compared to linear models (Guisan et al. 2002; Pearce et al. 2011; Wang et al. 2012).

2 Data and methods

2.1 Data

Datasets used in the study included the following: (1) the homogeneous, area-weighted time-series of annual summer (Jun–Sep) monsoon rainfall totals (JJAS) for the period 1871–2011 (Parthasarathy et al. 1994); (2) summer NINO4 (sea surface temperature (SST) averaged over 160°E–150°W and 5°S–5°N) which is an ENSO index based on the Extended Reconstructed SST dataset (Smith et al. 2008; ERSSTvb3); (3) the summer IOD index-difference in SST anomalies between the western (50°E–70°E and 10°S–10°N) and eastern (90°E–110°E and 10°S–0°S) tropical Indian Ocean (Saji et al. 1999), also computed using the ERSSTvb3 (4) the summer El Niño Modoki Index (EMI; Ashok et al. 2007)-difference in SST anomalies over three regions (165°E–140°W and 10°S–10°N; 110°W–70°W and 15°S–5°N; 125°E–145°E and 10°S–20°N) computed using the ERSSTvb3 (5) NINO4 and IOD indices from the Extended Kaplan SST (Kaplan et al. 1998) dataset and (6) daily gridded rainfall data over India for the period 1901–2004 (Rajeevan et al. 2006). From the latter, ERE frequencies—the number of days of rainfall exceeding a given threshold over all grids in India in each year—were determined. EREs are increasingly being defined in terms of their impacts in certain regions or under specific antecedent moisture conditions and the carrying capacity of the ecosystem rather than based only on absolute or relative values (Pielke and Downton 2000). For example, in the Himalayas, 25 mm day^{-1} is considered a critical threshold for the occurrence of major landslides once adequate antecedent moisture has accumulated (Gabet et al. 2004). Similarly, other global and regional studies, which define heavy and extreme precipitation for studying long-terms trends or impacts of climate change, have classified events of 25 mm day^{-1}as extreme events (Zhai et al. 2005; Hennessy et al. 1997; Groisman et al. 1999). In this work, the following exceedance thresholds were therefore selected: 25, 50, 100, 150 and 200 mm per day. The IM data was obtained from http://www.tropmet.res.in/and the indices from http://iridl.ldeo.columbia.edu/.

It is important to note that the NINO4 index was chosen based on recent results that showed this region in the equatorial Pacific to have a stronger teleconnection with the IM (Kumar et al. 2006; Rajagopalan and Molnar 2012). The sign of the index was reversed to give a positive correlation with IM rainfall for easier interpretation and comparison with influence of IOD, whose positive phase is associated with higher rainfall in IM. Positive values of the redefined NINO4 index thus correspond to the La Nina phase, which is associated with higher IM rainfall and potentially higher frequency of EREs and the lower negative end of the scale corresponds to the extreme El Nino phase.

3 Methods

3.1 Bayesian dynamic linear regression

In a traditional (or static) linear regression model, the regression coefficients estimated based on historical data do not change over time. In contrast, in dynamic linear models the regression coefficients such as intercepts and regression slopes can vary as a function of time, i.e. they allow us to capture the time-varying nature of the relationship. Dynamic linear models (Petris et al. 2009) consider a time series as the output of a dynamical system perturbed by random disturbances. This allows a robust quantification and elegant visualization of the changing influences of covariates. In Bayesian dynamic regression models (Harrison and West 1997; Petris et al. 2009), a type of dynamic state space model, regression coefficients are updated at each time step, conditional on available data and the model using Bayes theorem. The general form of the model is represented as

$$Y_t = \beta 0_t + \beta 1_t X1_t + \beta 2_t X2_t + \ldots + e_t \quad (1)$$

$$e_t \approx N(0, V)$$

where Y is the dependent variable (e.g., IM annual totals and square root of annual counts of EREs in this study) and $X1$, $X2$,… are the independent variables (e.g., NINO4 and IOD in this study), t denotes the time ($t = 1, 2,\ldots, N$) and $\beta 0_t$, $\beta 1_t$, $\beta 2_t$,… are the time varying intercept and slopes, respectively (i.e., regression coefficients). e_t is the noise or error distributed normally with a mean of 0 and variance V, and can be obtained from the residual variance from the traditional regression model fitted to the data. The time-varying intercept represents the level at time t corresponding to the covariate model. Its time-trajectory constitutes an overall level/trend that can be interpreted as variability in the response variable that is not captured by the covariates

alone. The trends in the time-varying slope can be directly interpreted as changes in the influence of that covariate on the response variable.

Equation 2 models the time varying regression coefficients—i.e., system dynamics. The parameter W which controls the dynamics of the time-evolution of the regression coefficients is specified a priori by setting W/V, the signal to noise ratio. As V is known (obtained from the residual error variance from a traditional regression), assuming the ratio W/V specifies W—a conservative value of 0.1 is adopted in our study.

$$\beta 0_t = \beta 0_{(t-1)} + w_t, \beta 1_t = \beta 1_{(t-1)} + w_t, \beta 2_t = \beta 2_{(t-1)} + w_t, \ldots, \text{where} \quad (2)$$

$$w_t \approx N(0, W)$$

The posterior predictive distribution of model coefficients at each time t is based on the distribution of coefficients from the previous time step t-1 (i.e., *prior*), and the probability of the data Y_t conditional on the model parameters at time t, (i.e., likelihood) using Bayes theorem as:

$$P(\theta_t|Y_t) \propto P(Y_t|\theta_t)P\left(\theta_t|Y_{(t-1)}\right) \quad (3)$$

where θ_t represents the vector containing the regression coefficients at time t.

At the start, the regression coefficients are estimated from a traditional static linear regression which provides the mean value and the variance of the coefficients with a normal distribution—i.e., $\theta_0 \approx N(m_0, C_0)$ where m_0 and C_0 are the mean vector and the variance–covariance matrix of the regression parameters. Posterior distributions of parameters at any time t can be obtained recursively using a Kalman filtering approach along with Markov chain Monte Carlo simulation approach. Bayesian confidence intervals can be generated from the posterior distributions. Here, we used the library *dlm* in R (Petris et al. 2009).

Although in this study we used a retrospective analysis, DLMs can also be used in forecasting and predictions at time $t + k$ using the regression models conditioning on information known up to a particular time period t.

One of the advantages of DLMs is that they offer a frame-work for prediction and forecasting as well, which a moving window correlation cannot. Their ability to have both time-varying intercept and slopes in the model makes it easier to attribute linkages of the response to not only the covariates but also to unmodeled factors. In addition, since a bayesian updating of model parameters evolves

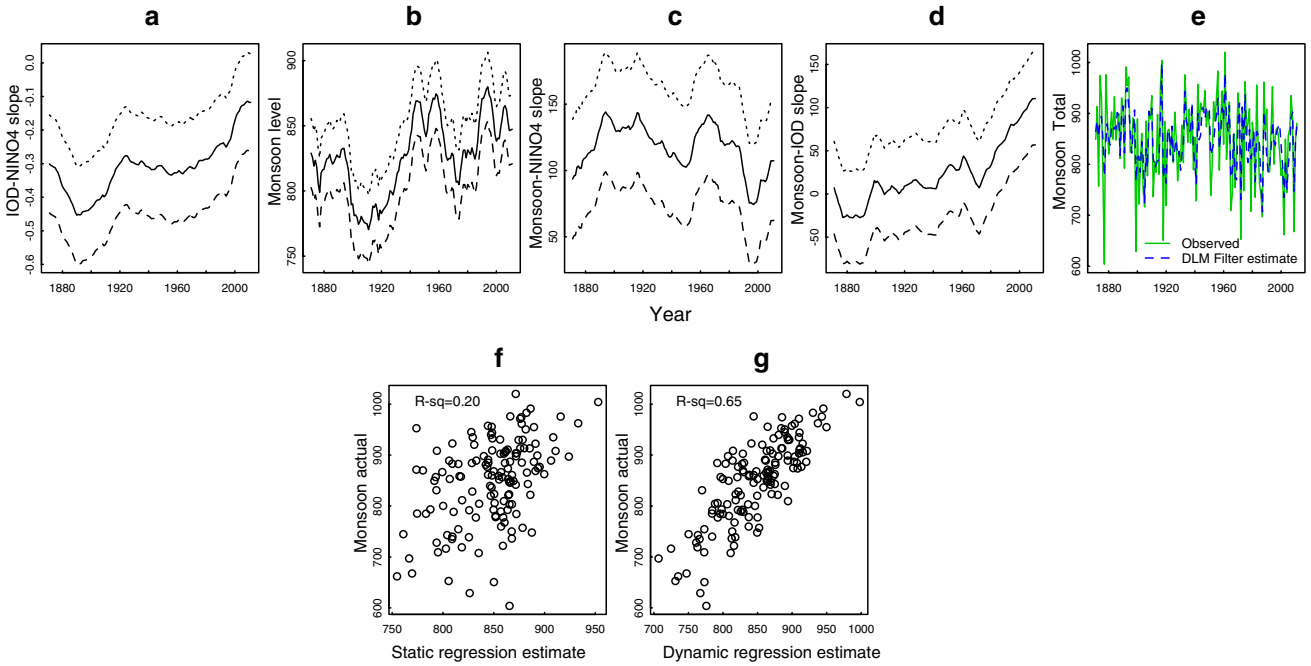

Fig. 1 Changes in the relationship between IOD and NINO4, and the relationships between these indices and the Indian monsoon over time. Each plot includes a regression parameter (intercept or slope; *solid line*) along with the 25th and 75th percentile credible interval lines (*dotted lines*) estimated using dynamic regression models. **a** Plot of the time-varying slope of the relationship between NINO4 and IOD, **b** Time varying intercept (monsoon level) for the regression of IM with NINO4 and IOD as co-variates, **c** Time-varying slope of the IM–NINO4 relationship, **d** Time varying slope of the IM–IOD relationship, and **e** plot of the estimated rainfall from the dynamic regression model (*dotted blue line*) and the observed rainfall (*solid green line*) over time. **f** Actual and estimated monsoon totals using the ordinary static regression model. **g** Actual and estimated monsoon totals using the dynamic regression model. p values for regression model in **f** and **g** are less than 0.0001

through the time-series, the transition across major changes, whether abrupt or gradual is easily captured.

3.2 Generalized additive model (GAM)

Generalised Additive Models were used to detect nonlinearities that might be present in the relationship between covariates (NINO4 and IOD) and monsoon attributes (IM totals, annual frequency of EREs), which are typically hard to capture using traditional linear regression methods. The general form of these models used were:

$$g(E(Y_t)) = \beta_0 + f_1(X_{1t}) + f_2(X_{2t}) \quad (4)$$

The function $g(.)$ is the link function. The functions f_i for each variable X_i used was nonparametric–splines, thus providing the ability to capture appropriate levels of nonlinearities in these variables. The smoothing function for each predictor is derived separately from the data and these are combined additively to generate the fitted values. The covariate range is covered using knots which define segments where the local spline functional form is fitted to define the response. In the case of Y being the monsoon totals, the covariates were the monsoon seasonal average NINO4 and IOD indices for each year and, we used the identity link and Gaussian distribution for the error. In the case of EREs the response variables, Y, are the square transformed counts of monsoon seasonal EREs in each year at different exceedance thresholds and the covariates were the same as described above. However, the link function chosen was the log, the standard link function for Poisson distribution appropriate for count data, such as the case here. The difficulty in specifying a probability distribution for the response and error terms is overcome by the use of quasi-likelihood models where only a relationship between mean and variance is specified, and the variance or dispersion is derived from the data. Therefore GAM models are very flexible in accommodating different distributions within the same broad family (i.e. Poisson in the case of count data).The p values obtained from the GAM models are based on the chi square distribution. GAM models are very flexible in being able to accommodate a variety of non-linear shapes and thus are particularly suitable for studying teleconnections between ocean–atmosphere phenomena and climate as these are non-linear and complex (Hoerling et al. 1997).

The output of the GAM models included the fitted values obtained as the expected value of the counts using back-transformation using the link function. The fitted values can be plotted against the covariates and the uncertainty in the scatter quantified using non-parametric smoothing method using the qplot function in R. This enables the interpretation of the response variable in the original units. Uncertainty in fitted GAM models was assessed in two distinct ways: p values from the GAM models, as well as visual interpretation of standard error bands on the fitted values plotted against the individual covariate.

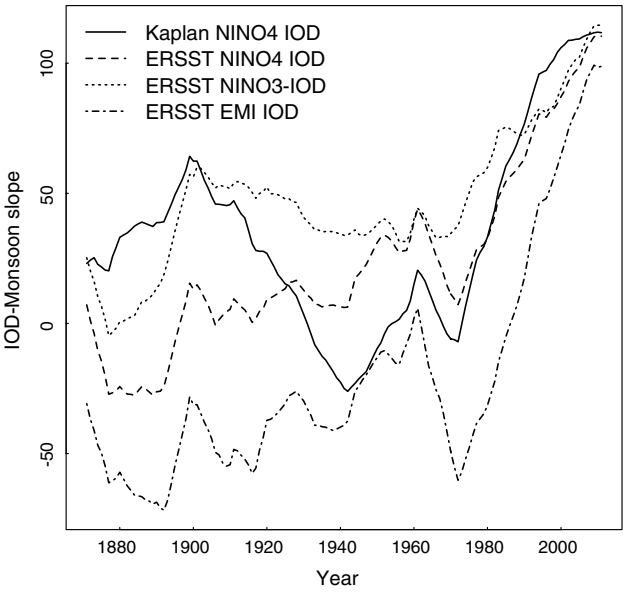

Fig. 2 Time-varying regression slope coefficient of monsoon-Indian Ocean Dipole (IOD) from dynamic linear models in which the annual Monsoon totals were regressed against NINO indices from different sources and corresponding IOD indices. Note the increase in the monsoon-IOD slope in recent decades across various SST sources and indices

4 Results and discussion

We fitted a DLM to IOD with NINO4 as the covariate to investigate the changing relationship between these two indices. Results (Fig. 1a) show a generally negative slope suggesting that that the La Nina phase of NINO4 and the positive IOD positive do not co-occur. It also suggests that IOD's correlation with NINO4 may be weakening in the last decade, indicated by the time-varying slopes tending towards zero. A DLM was fitted to IM as a function of NINO4 and IOD. The time varying intercept (or level) is shown in Fig. 1b, which shows multi-decadal variability with three peaks and troughs. Further, such variability is consistent with multi-decadal variability of the IM rainfall documented by others (e.g., Ummenhofer et al. 2011). The slope of IM–NINO4 shows a recent recovery from the decline from 1960s (Fig. 1c), but the most interesting and clear trend is in the IM–IOD slope which shows a consistent increase since the 1960s (Fig. 1d). Thus, a unit change in IOD is producing proportionately more impacts on the IM relative to earlier periods. Interestingly, the period since 1960s is also the period for which a reduced

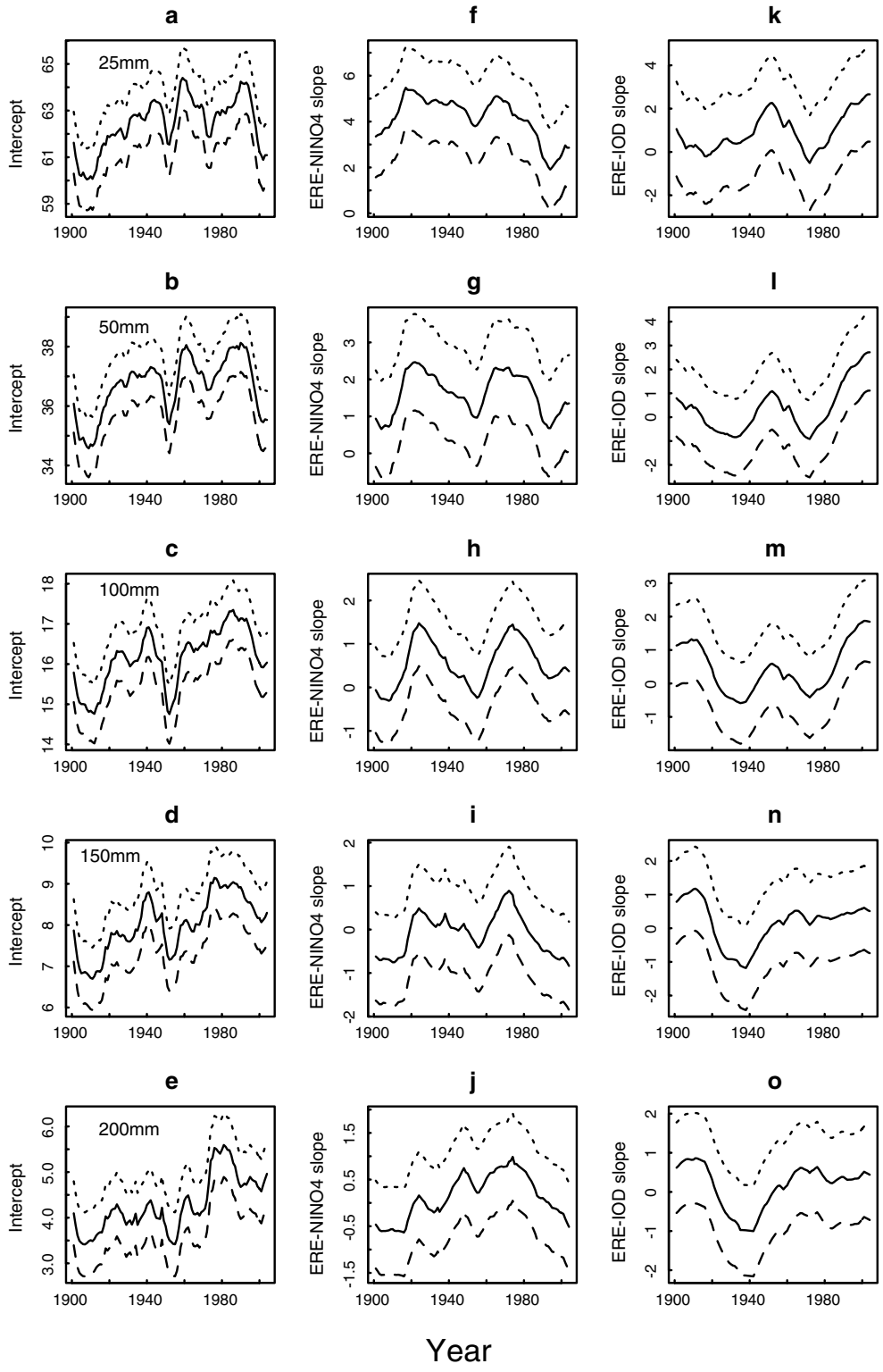

Fig. 3 Time-varying influence of NINO4 and IOD on the annual counts of EREs (square root transformed) for the periods 1901–2004 at different daily exceedance thresholds (25, 50, 100,150 and 200 mm). The time-varying level and regression slope coefficients are plotted (*solid line*) along with 25th and 75th intervals (*dotted lines*). The first column **a**–**e** plots the time-varying level or intercept. The third column **f**–**j** show the time-varying regression slope coefficient of ERE with NINO4, while the last column **k**–**o** shows the regression coefficient slope of ERE against IOD. Note the increasing influence of IOD in recent decades relative to earlier periods

monsoon-ENSO relationship was reported (Kumar et al. 1999). The mean estimates of IM from the dynamic regression model capture the observed variations in the IM quite well (Fig. 1e). Furthermore, this model outperforms traditional linear regression models (Fig. 1f, g). Additionally, the results were verified using the Kaplan SST dataset for NINO4 and IOD. We also used the NINO3 and EMI indices derived from ERSSTvb3, to verify the increasing influence of IOD on the IM (Fig. 2). Despite some differences, the overall trends and patterns in results are robust over different SST sources and ENSO indices, suggesting the increasing influence of IOD on the IM.

A dynamic regression model was applied to ERE counts at various thresholds and the time varying coefficients are shown in Fig. 3. The time-varying regression intercept (Fig. 3a–e) indicates multi-decadal variability and highlights an overall increasing trend in EREs of 150 and 200 mm exceedance since the early 1900s, however there is a lot of variability in recent decades. Earlier studies across multi-decadal scales have shown a similar increasing trend in EREs over the Indian subcontinent (Goswami et al. 2006; Rajeevan et al. 2008). The time varying slopes of NINO4 and IOD can be seen in Fig. 3f–j and k–o, respectively. The influence of IOD has been increasing, while that of NINO4 has been declining, over the last few decades, particularly for the higher exceedance thresholds. The non-stationarity in the influence of NINO4 and IOD on the IM and corresponding EREs is quite clear from DLM—they both point to an increasing influence of IOD on EREs since the 1940s with the slope changing from negative to positive, albeit with a high degree of uncertainty. The influence of IOD on EREs remains consistent across different sources of SST and ENSO indices (Fig S1).

The non-linear relationship between NINO4 and IOD with IM totals was explored by fitting a GAM (Fig. 4, Fig S2 and S3). Based on the DLM analysis, the early 1940s emerged as a turning point in the relationship between frequency of EREs and IOD (Fig. 3). We thus explored the non-linearity of the IM total NINO4–IOD relationships in the two periods preceding and after the year 1941. The associated p values from the GAM models and standard errors of the fitted values clearly highlight that that the relationships between ENSO and IOD indices and IM changed after the 1940s (Fig. 4, Fig S2 and Fig S3). A similar changing influence of IOD on EREs (above 150 mm) is also evident during the second half (1942–2011) of the study period (Fig. 3n–o and Fig S1). The changing influence of ENSO and IOD on IM since 1940s remains consistent across different types of ENSO indices. However, this is not necessarily true across different SST sources (Fig. 3 and Fig S3). Overall, it's evident that the influence of IOD has strengthened in the 1942–2011 period compared to ENSO, whose relationship with IM seems to be more uncertain and more non-linear relative to 1871–1941 period.

In order to investigate the nature of relationship between NINO4 and IOD with EREs, a GAM was fitted to the ERE counts for different thresholds (Fig. 5). As the number EREs are sparse, especially for higher exceedance thresholds, we applied the GAM model to data from the entire time-period (1901–2007). For lower exceedance thresholds (25, 50 mm day^{-1}), IOD has an influence on frequency of EREs only in its positive phase, but for higher exceedance thresholds, the positive influence of IOD is evident across the range of the IOD index values (Fig. 5 and Fig S4). Thus, IOD is more important for influencing EREs at higher exceedance levels. Furthermore, for the higher exceedance EREs there is a pronounced non-linear dip in the influence of IOD at the higher end, possibly suggesting

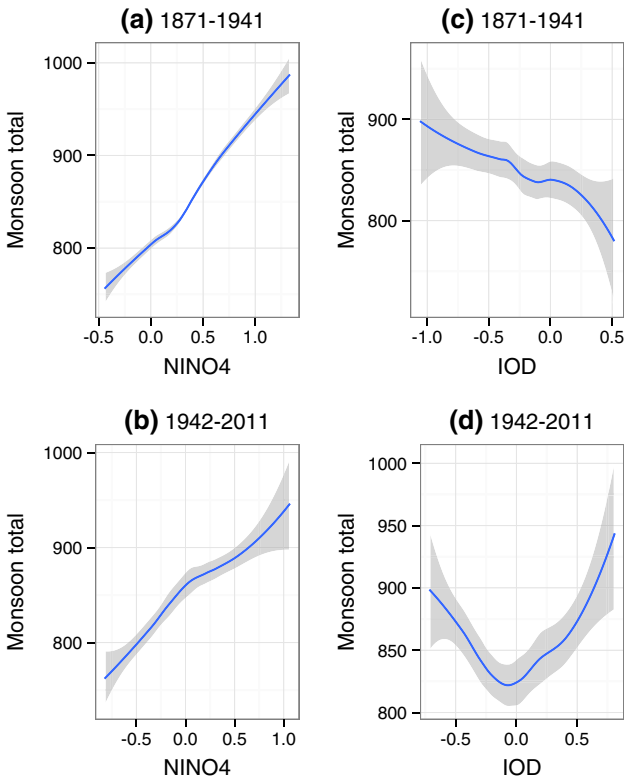

Fig. 4 Non linear response of annual IM totals to NINO4 and IOD. Modelled IM total as a function of NINO4 (**a**–**b**) and IOD (**c**–**d**). The *solid lines* represent the fitted values of IM total as a function of either NINO4 or IOD based on generalized additive modelling, while the *shaded areas* represent the standard error bands. IOD emerges as the more monotonic and consistent driver of IM especially in the recent decades. The associated p value of GAM model was significant ($p < 0.03$) for influence of IOD for the period 1942–2011, however the standard error bands on the fitted values suggests shifts in the relative role of NINO4 and IOD on the IM between 1942–2011 relative to the earlier period

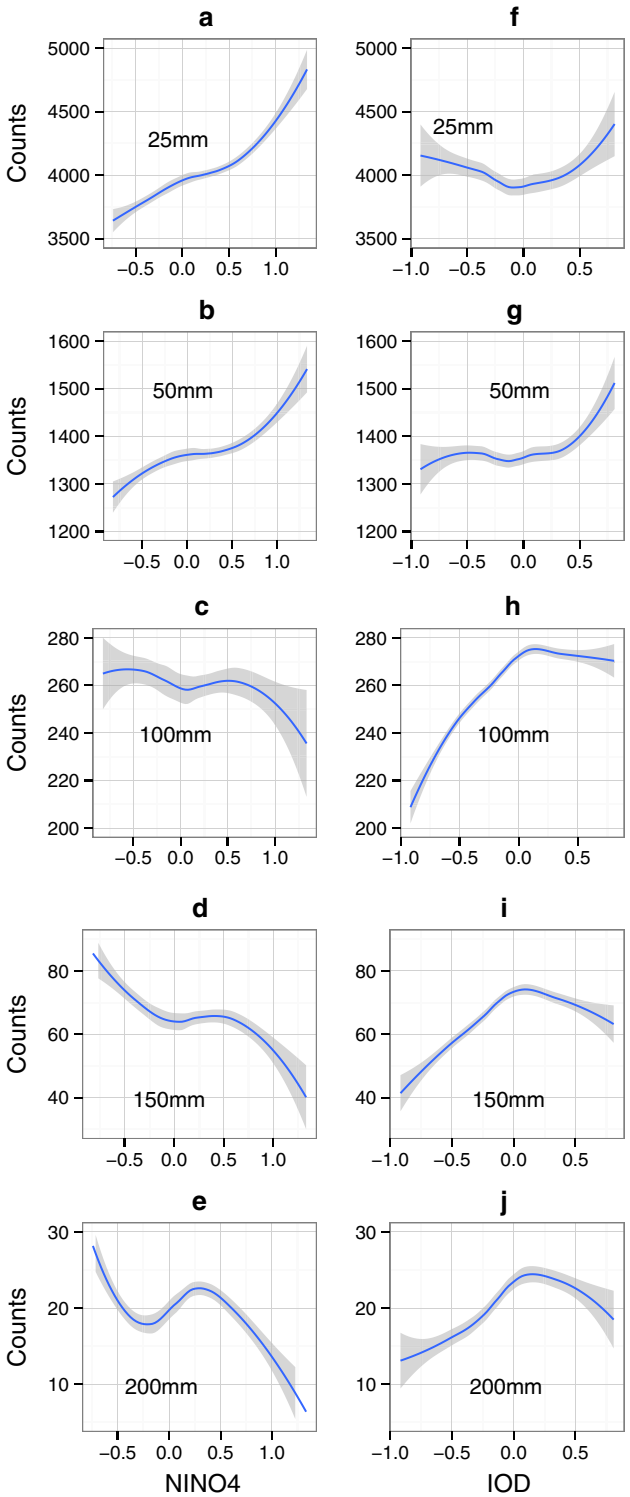

Fig. 5 Non linear response of ERE counts to NINO4 and IOD. Modelled ERE counts as a function of NINO4 (**a**–**e**) and IOD (**f**–**j**) for time periods 1901–2004 for rainfall exceedance thresholds of 25 mm (row 1), 50 mm (row 2), 100 mm (row 3), 150 mm (row 4) and 200 mm (row 5). The *solid lines* represent the fitted values of ERE counts as a function of either NINO4 or IOD based on generalized additive modelling, while the *shaded areas* represent the standard error bands. IOD emerges as the more monotonic and consistent driver of EREs especially at higher exceedance thresholds. All models are significant at $p < 0.001$

the inhibiting influence of un-modelled processes or the influence of different physical processes when compared to lower thresholds.

Nonlinearities in the relationships are quite apparent from these plots. Positive values of IOD are generally associated with an increase in ERE counts (all results were significant at $p < 0.001$), but for 100 mm and above EREs increase with the IOD index, but flatten out at positive IOD values, suggesting that local or regional drivers in addition to the two ocean–atmosphere phenomena could be influencing occurrence of very high EREs. The spatial distribution of high EREs (Fig S5) indicates that large areas in India (including upper catchments of major rivers) are prone to flooding. Such areas also incorporate large vulnerable populations including major urban centres. Also in urban landscapes pluvial flooding is a major source of concern and can occur at lower rain intensities (Dawson et al. 2008). As urbanization spreads, vulnerability is predicted to increase in these regions.

The DLM and GAM methods provide a robust approach to modelling non-stationarity and nonlinearity in relationships between large climate features and regional precipitation as well as quantifying the uncertainties. Our approaches can be applied to other regions where ocean–atmosphere phenomenon is known to influence precipitation, and thus evaluate any changes in the pattern of rainfall and EREs. Such analysis should be informed by a comparison across different SST sources used for defining ocean–atmosphere indices. This is especially important as the uncertainty about SST data before 1950 is higher.

Our research and results highlight several exciting and challenging questions. Can dynamic models that include IOD as a covariate improve the predictability of monsoon rainfall and its extremes at time-scales finer than annual? Can we map spatially explicit influences of ENSO and IOD for larger regions to identify vulnerable and sensitive areas? Can we identify local and regional factors that influence EREs apart from ocean–atmosphere phenomena? Can long term simulations from GCM models confirm the shifts in the relative role of ENSO and IOD on the IM? The impact of changing climate and weather extremes on future socio-economic welfare and ecosystem responses in India and elsewhere is a major area of concern for adaptation strategies (Easterling et al. 2000; Meehl et al. 2000; Kundzewicz et al. 2008; Revi 2008; Tubiello et al. 2007). Clearly, advances in these questions will make a meaningful difference to the region's social and economic well-being and the sustainability of its ecosystems and ecosystem services.

Acknowledgments We would like to thank the jointly administered Changing Water Cycle programme of the Ministry of Earth Sciences (Grant Ref: MoES/NERC/16/02/10 PC-11), Government of India and Natural Environment Research Council (Grant Ref: NE/I022450/1), United Kingdom for financial support. We thank the two anonymous reviewers and editor for their helpful comments and suggestions on an earlier version of this article. We dedicate this paper to our colleague and co-author Professor Mike Bonell who passed away on July 11th, 2014.

References

Abram NJ, Gagan MK, Cole JE, Hantoro WS, Mudelsee M (2008) Recent intensification of tropical climate variability in the Indian Ocean. Nat Geosci 1:849–853. doi:10.1038/ngeo357

Ajaymohan RS, Rao SA (2008) Indian Ocean dipole modulates the number of extreme rainfall events over india in a warming environment. J Meteorol Soc Jpn Ser II 86:245–252

Ashfaq M, Shi Y, Tung W, Trapp RJ, Gao X, Pal JS, Diffenbaugh NS (2009) Suppression of south Asian summer monsoon precipitation in the 21st century. Geophys Res Lett 36:L01704. doi:10.1029/2008GL036500

Ashok K, Saji NH (2007) On the impacts of ENSO and Indian Ocean dipole events on sub-regional Indian summer monsoon rainfall. Nat Hazards 42:273–285. doi:10.1007/s11069-006-9091-0

Ashok K, Guan Z, Yamagata T (2001) Impact of the Indian Ocean dipole on the relationship between the Indian monsoon rainfall and ENSO. Geophys Res Lett 28:4499–4502

Ashok K, Guan Z, Saji NH, Yamagata T (2004) Individual and combined influences of ENSO and the Indian Ocean dipole on the Indian summer monsoon. J Clim 17:3141–3155

Ashok K, Behera SK, Rao SA, Weng H, Yamagata T (2007) El Niño Modoki and its possible teleconnection. J Geophys Res 112:C11007

Ashrit RG, Kumar KR, Kumar KK (2001) ENSO-monsoon relationships in a greenhouse warming scenario. Geophys Res Lett 28:1727–1730

Cai W, Cowan T, Sullivan A (2009) Recent unprecedented skewness towards positive Indian Ocean dipole occurrences and its impact on Australian rainfall. Geophys Res Lett 36:L11705

Calder C, Lavine M, Müller P, Clark JS (2003) Incorporating multiple sources of stochasticity into dynamic population models. Ecology 84(6):1395–1402

Cherchi A, Navarra A (2013) Influence of ENSO and of the Indian Ocean Dipole on the Indian summer monsoon variability. Clim Dyn 41:81–103. doi:10.1007/s00382-012-1602-y

Dawson R, Speight L, Hall J, Djordjevic S, Savic D, Leandro J (2008) Attribution of flood risk in urban areas. J Hydroinformatics 10:275–288

Easterling DR, Meehl GA, Parmesan C, Changnon SA, Karl TR, Mearns LO (2000) Climate extremes: observations, modeling, and impacts. Science 289:2068–2074. doi:10.1126/science.289.5487.2068

Gabet EJ, Burbank DW, Putkonen JK, Pratt-Sitaula BA, Ojha T (2004) Rainfall thresholds for landsliding in the Himalayas of Nepal. Geomorphology 63:131–143

Gadgil S, Kumar KR (2006) The Asian monsoon—agriculture and economy. Asian Monsoon. Springer, Berlin Heidelberg, pp 651–683

Ghosh S, Das D, Kao S-C, Ganguly AR (2012) Lack of uniform trends but increasing spatial variability in observed Indian rainfall extremes. Nat Clim Change 2:86–91. doi:10.1038/nclimate1327

Goswami BN, Venugopal V, Sengupta D, Madhusoodanan MS, Xavier PK (2006) Increasing trend of extreme rain events over India in a warming environment. Science 314:1442–1445

Groisman P, Karl T, Easterling D, Knight R, Jamason P, Hennessy K, Suppiah R, Page C, Wibig J, Fortuniak K, Razuvaev V, Douglas A, Førland E, Zhai P-M (1999) Changes in the probability of heavy precipitation: important indicators of climatic change. Clim Change 42:243–283. doi:10.1023/A:1005432803188

Guhathakurta P, Rajeevan M (2008) Trends in the rainfall pattern over India. Int J Climatol 28:1453–1469

Guhathakurta P, Sreejith O, Menon PA (2011) Impact of climate change on extreme rainfall events and flood risk in India. J Earth Syst Sci 120:359–373. doi:10.1007/s12040-011-0082-5

Guisan A, Edwards TC Jr, Hastie T (2002) Generalized linear and generalized additive models in studies of species distributions: setting the scene. Ecol Model 157:89–100

Han W, Meehl GA, Rajagopalan B, Fasullo JT, Hu A, Lin J, Large WG, Wang J, Quan X-W, Trenary LL, Wallcraft A, Shinoda T, Yeager S (2010) Patterns of Indian Ocean sea-level change in a warming climate. Nat Geosci 3:546–550. doi:10.1038/ngeo901

Harrison J, West M (1997) Bayesian forecasting and dynamic models. Springer Verlag, New York

Harrisons PJ, Stevens CF (1976) Bayesian forecasting (with discussion). J Roy Stat Soc Ser B 38:205–247

Hastie T, Tibshirani R (1986) Generalized additive models. Stat Sci 1:297–310. doi:10.1214/ss/1177013604

Hastie T, Tibshirani R (1990) Generalized additive models. Chapman & Hall/CRC, Florida

Hennessy KJ, Gregory JM, Mitchell JFB (1997) Changes in daily precipitation under enhanced greenhouse conditions. Clim Dyn 13:667–680. doi:10.1007/s003820050189

Hoerling MP, Kumar A, Zhong M (1997) El Niño, La Niña, and the nonlinearity of their teleconnections. J Clim 10:1769–1786. doi:10.1175/1520-0442(1997)010<1769:ENOLNA>2.0.CO;2

Ihara C, Kushnir Y, Cane MA (2008) Warming trend of the indian ocean SST and Indian Ocean dipole from 1880 to 2004. J Clim 21:2035–2046

Izumo T, Vialard J, Lengaigne M, de Boyer Montegut C, Behera SK, Luo J–J, Cravatte S, Masson S, Yamagata T (2010) Influence of the state of the Indian Ocean dipole on the following year/'s El Nino. Nat Geosci 3:168–172. doi:10.1038/ngeo760

Kaplan A, Cane MA, Kushnir Y, Clement AC, Blumenthal MB, Rajagopalan B (1998) Analyses of global sea surface temperature 1856–1991. J Geophys Res Oceans 103:18567–18589. doi:10.1029/97JC01736

Krishnan R, Sabin TP, Ayantika DC, Kitoh A, Sugi M, Murakami H, Turner AG, Slingo JM, Rajendran K (2013) Will the South Asian monsoon overturning circulation stabilize any further? Clim Dyn 40:187–211. doi:10.1007/s00382-012-1317-0

Krishnaswamy J, Lavine M, Richter DD, Korfmacher K (2000) Dynamic modeling of long-term sedimentation in the Yadkin River basin. Adv Water Resour 23:881–892. doi:10.1016/S0309-1708(00)00013-0

Krishnaswamy J, Halpin PN, Richter DD (2001) Dynamics of sediment discharge in relation to land-use and hydro-climatology in a humid tropical watershed in Costa Rica. J Hydrol 253:91–109. doi:10.1016/S0022-1694(01)00474-7

Krishnaswamy J, John R, Joseph S (2014) Consistent response of vegetation dynamics to recent climate change in tropical mountain regions. Glob Change Biol 20:203–215. doi:10.1111/gcb.12362

Kumar KK, Rajagopalan B, Cane MA (1999) On the weakening relationship between the Indian monsoon and ENSO. Science 284:2156–2159

Kumar KK, Rajagopalan B, Hoerling M, Bates G, Cane M (2006) Unraveling the mystery of Indian monsoon failure during El Niño. Science 314:115–119

Kumar KK, Kamala K, Rajagopalan B, Hoerling M, Eischeid J, Patwardhan SK, Srinivasan G, Goswami BN, Nemani R (2011) The

once and future pulse of Indian monsoonal climate. Clim Dyn 36:2159–2170. doi:10.1007/s00382-010-0974-0

Kundzewicz ZW, Mata LJ, Arnell NW, Döll P, Jimenez B, Miller K, Oki T, Şen Z, Shiklomanov I (2008) The implications of projected climate change for freshwater resources and their management. Hydrol Sci J 53:3–10. doi:10.1623/hysj.53.1.3

Lehmann A, Overton JM, Austin MP (2002) Regression models for spatial prediction: their role for biodiversity and conservation. Biodivers Conserv 11:2085–2092. doi:10.1023/A:1021354914494

Luo J-J, Zhang R, Behera SK, Masumoto Y, Jin F-F, Lukas R, Yamagata T (2010) Interaction between El Niño and extreme Indian Ocean dipole. J Clim 23:726–742. doi:10.1175/2009JCLI3104.1

Maity R, Nagesh Kumar D (2006) Bayesian dynamic modeling for monthly Indian summer monsoon rainfall using El Niño–Southern Oscillation (ENSO) and Equatorial Indian Ocean Oscillation (EQUINOO). J Geophys Res Atmos 111:D07104. doi:10.1029/2005JD006539

Meehl GA, Karl T, Easterling DR, Changnon S, Pielke R, Changnon D, Evans J, Groisman PY, Knutson TR, Kunkel KE, Mearns LO, Parmesan C, Pulwarty R, Root T, Sylves RT, Whetton P, Zwiers F (2000) An introduction to trends in extreme weather and climate events: observations, socioeconomic impacts, terrestrial ecological impacts, and model projections. Bull Am Meteorol Soc 81:413–416. doi:10.1175/1520-0477(2000)081<0413:AITTIE>2.3.CO;2

Parthasarathy B, Munot AA, Kothawale DR (1994) All-India monthly and seasonal rainfall series: 1871–1993. Theor Appl Climatol 49:217–224. doi:10.1007/BF00867461

Pearce JL, Beringer J, Nicholls N, Hyndman RJ, Tapper NJ (2011) Quantifying the influence of local meteorology on air quality using generalized additive models. Atmos Environ 45:1328–1336. doi:10.1016/j.atmosenv.2010.11.051

Petris G, Petrone S, Campagnoli P (2009) Dynamic linear models. Dyn. Linear Models R. Springer: New York, pp 31–84

Pielke RA, Downton MW (2000) Precipitation and damaging floods: trends in the United States, 1932–97. J Clim 13:3625–3637. doi:10.1175/1520-0442(2000)013<3625:PADFTI>2.0.CO;2

Prajeesh AG, Ashok K, Rao DVB (2013) Falling monsoon depression frequency: A Gray-Sikka conditions perspective. Sci Rep 3

Rajagopalan B, Molnar P (2012) Pacific Ocean sea-surface temperature variability and predictability of rainfall in the early and late parts of the Indian summer monsoon season. Clim Dyn 39:1543–1557. doi:10.1007/s00382-011-1194-y

Rajeevan M, Bhate J, Kale JD, Lal B (2006) High resolution daily gridded rainfall data for the Indian region: analysis of break and active monsoon spells. Curr Sci 91:296–306

Rajeevan M, Bhate J, Jaswal AK (2008) Analysis of variability and trends of extreme rainfall events over India using 104 years of gridded daily rainfall data. Geophys Res Lett 35:L18707

Revi A (2008) Climate change risk: an adaptation and mitigation agenda for Indian cities. Environ Urban 20:207–229. doi:10.1177/0956247808089157

Saji NH, Goswami BN, Vinayachandran PN, Yamagata T (1999) A dipole mode in the tropical Indian Ocean. Nature 401:360–363. doi:10.1038/43854

Smith TM, Reynolds RW, Peterson TC, Lawrimore J (2008) Improvements to NOAA's historical merged land-ocean surface temperature analysis (1880–2006). J Clim 21:2283–2296

Trenberth KE, Dai A, Rasmussen RM, Parsons DB (2003) The changing character of precipitation. Bull Am Meteorol Soc 84:1205–1217. doi:10.1175/BAMS-84-9-1205

Tubiello FN, Soussana J-F, Howden SM (2007) Crop and pasture response to climate change. Proc Natl Acad Sci 104:19686–19690. doi:10.1073/pnas.0701728104

Turner AG, Annamalai H (2012) Climate change and the South Asian summer monsoon. Nat Clim Change 2:587–595. doi:10.1038/nclimate1495

Ummenhofer CC, Gupta AS, Li Y, Taschetto AS, England MH (2011) Multi-decadal modulation of the El Nino–Indian monsoon relationship by Indian Ocean variability. Environ Res Lett 6:034006

Vinayachandran PN, Francis PA, Rao SA (2009) Indian Ocean dipole: Processes and impacts. In: Mukunda, N. (ed) Current trends in science, platinum jubilee special. Indian Academy of Sciences, pp 569–589

Wang X, Wang C (2014) Different impacts of various El Niño events on the Indian Ocean dipole. Clim Dyn 42(3–4):991–1005

Wang P, Baines A, Lavine M, Smith G (2012) Modelling ozone injury to U.S. forests. Environ Ecol Stat 19:461–472. doi:10.1007/s10651-012-0195-2

Wang B, Yim S-Y, Lee J-Y, Liu J, Ha K-J (2013) Future change of Asian-Australian monsoon under RCP 4.5 anthropogenic warming scenario. Clim Dyn 42:83–100. doi:10.1007/s00382-013-1769-x

West M, Harrison PJ, Migon HS (1985) Dynamic generalized linear models and bayesian forecasting. J Am Stat Assoc 80:73–83. doi:10.1080/01621459.1985.10477131

Yee TW, Mitchell ND (1991) Generalized additive models in plant ecology. J Veg Sci 2:587–602. doi:10.2307/3236170

Zhai P, Zhang X, Wan H, Pan X (2005) Trends in total precipitation and frequency of daily precipitation extremes over China. J Clim 18:1096–1108. doi:10.1175/JCLI-3318.1